MATERIAL INDUCED ANISOTROPIC DAMAGE

Muhammad S. Niazi[1*], Hendrik H. Wisselink[1], Timo Meinders[2], Antonius H. van den Boogaard[2]

[1]Materials innovation institute, 2600 GA Delft, The Netherlands
[2]University of Twente, 7500 AE Enschede, The Netherlands

ABSTRACT: The anisotropy in damage can be driven by two different phenomena; anisotropic deformation state named Load Induced Anisotropic Damage (LIAD) and anisotropic (shape and/or distribution) second phase particles named Material Induced Anisotropic Damage (MIAD). Most anisotropic damage models are based on LIAD. This work puts emphasis on the presence of MIAD in DP600 steel. Scanning Electron Microscopic (SEM) analysis was carried out on undeformed and deformed tensile specimens. The martensite morphology showed anisotropy in size and orientation. Consequently, significant MIAD was observed in the deformed tensile specimens. A through thickness shear failure is observed in the tensile specimen, which is pulled along the rolling direction (RD), whereas a dominant ductile fracture is observed when pulled perpendicular to RD. The Modified Lemaitre's (ML) anisotropic damage model is improved to account for MIAD in a phenomenological manner. The MIAD parameters are determined from tensile tests carried out in 0^o, 45^o and 90^o to the RD. The formability of DP600 is lower in the RD compared to that in 90^o to the RD, due to the phenomenon of MIAD.

KEYWORDS: Material induced anisotropic damage (MIAD), dual phase steels, martensite morphology

1 INTRODUCTION

In general, the process of damage is anisotropic [1]. The anisotropy in damage can be driven by two different phenomena; anisotropic deformation state i.e. Load Induced Anisotropic Damage (LIAD) and anisotropic second phase particles i.e. Material Induced Anisotropic Damage (MIAD) [2]. LIAD is related to the loading direction of the material. Generally damage grows faster in the direction of maximum principal stress irrespective of the anisotropy in the second phase particles and/or microstructure. The schematic in Fig. 1 shows how the stress state induces anisotropy in void growth. MIAD is a phenomenon in which the damage behavior of the material changes when material orientation is changed under the same loading conditions. Fig. 2 shows the SEM images during a scoring process. In the top image the RD is in plane while the transverse direction is out of plane. Coalescence of voids is observed in this case. In the bottom image, the transverse direction is in plane while the RD is out of plane. On contrary, no coalescence is observed in this case. In this example, the damage behavior is different when the material is oriented differently. This difference in damage behavior is attributed to the anisotropy of second phase particles or inclusions in the material. In DP600, martensite morphology is the main aspect which can lead to MIAD in this material.

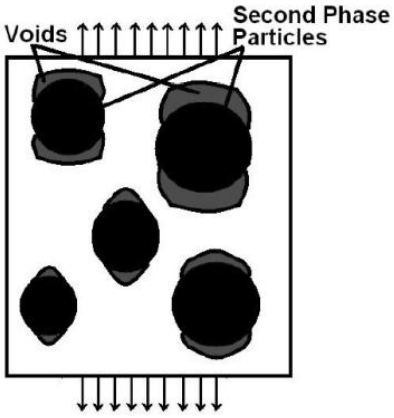

Fig. 1 *LIAD Schematic.*

Recently Avramovic-Cingara [3] studied the damage behavior in two different kinds of DP600 steel grades using metallographic (SEM) analysis. Different damage behavior was observed in both materials, which was clearly linked with the martensite morphology. In the article at hand, MIAD is studied in deformed DP600 tensile specimen, pulled in 0o and 90o to the RD, using SEM. The difference in damage / failure behavior is related to the difference in the martensite morphology in the two orientations. A MIAD model has been formulated using the modified Lemaitre's anisotropic damage model [2]. The MIAD model parameters are fitted to the tensile experiments.

* Corresponding author: P.O. Box. 5008, 2600GA Delft, The Netherlands, Ph.: +31534894175, m.niazi@m2i.nl

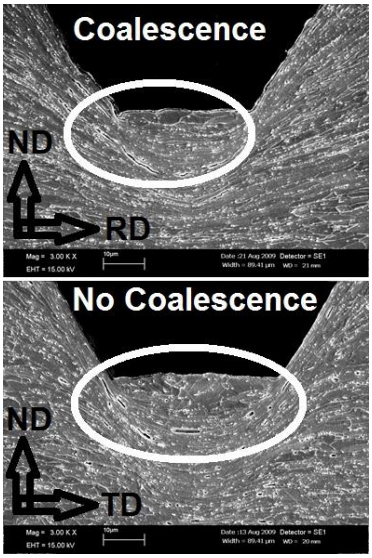

Fig. 2 *MIAD Example. (Courtesy Tata Steel)*

2 MOTIVATION

A stark difference was found in the results obtained from the tensile tests, carried out in 0^o and 90^o to RD. The material is plastically isotropic as the R-value (Lankford's coefficient) is approximately equal to 1 for this material. The material loaded in the RD fails approximately at 23% engineering strain whereas the material loaded in the 90^o to RD fails approximately at 26% engineering strain. These values are measured with a gauge length of 50mm. The stress level at which the material fails is approximately the same for both directions. Difference was also observed in the deformation characteristics and failure modes in the tests in 0^o and 90^o to RD. Fig. 3 shows the images of broken specimens in 0^o and 90^o to RD. At the lower left corner of the images, the major strain distribution (obtained by the ARAMIS system) just before failure, is shown. Difference can be observed in the failure angle, the fracture profile through thickness, the localization region and the strain gradient in the localized band. These differences motivated to study the martensite morphology and the failure with reference to MIAD.

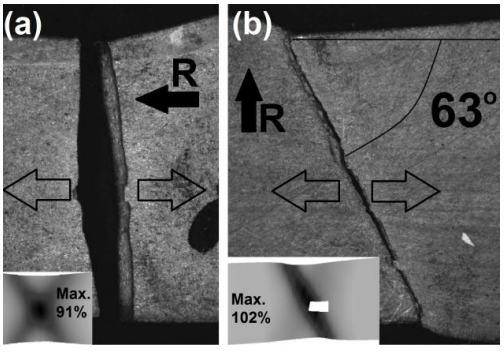

Fig. 3 *Difference in deformation and failure for specimen loaded in (a) 0^o (b) 90^o to RD.*

3 METALLOGRAPHY

3.1 UNDEFORMED MATERIAL

Fig. 4 shows the SEM images in the mid plane region along the thickness for the undeformed material. It is found that the martensite is more concentrated in the central region along the thickness in both 0^o to and 90^o to RD. This martensite is mainly in the form of bands. In the RD, Fig. 4(a), these bands are continuous and much longer compared to the bands in the 90^o to RD, Fig. 4(b). The central bands in the RD are 0.5-1.0 mm long whereas in the 90^o to RD these are utmost a couple of hundred microns. The average size of these bands is very important in determining the deformation and damage behavior in this material, especially, in the later stages of deformation i.e. when the strain localization length scale approaches the average size of these bands.

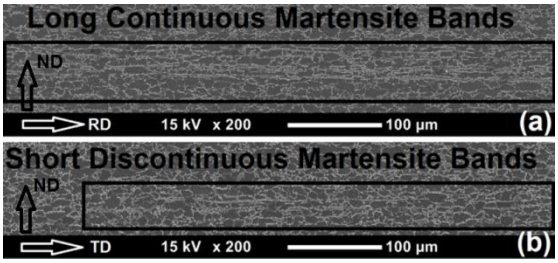

Fig. 4 *SEM images of undeformed DP600.*

3.2 DEFORMED UNBROKEN SAMPLES

SEM analysis was performed on unbroken samples, which are deformed beyond localization. Two samples were analyzed for each direction; one sample cut along the loading direction and the other perpendicular to the loading direction. The cuts were made in such a way that the surface crosses the maximum strain region. The strain level at the section was calculated by measuring the minimum thickness.

3.2.1 Specimens Loaded in RD

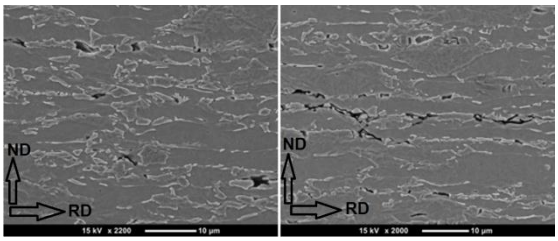

Fig. 5 *Sample cut ∥ to the loading direction.*

Fig. 5 shows the SEM images in the central martensite band region for the sample cut along the loading direction. The left image shows that the central martensite band is getting fractured at random intervals and thus voids are being produced. The right image shows some hints of coalescence

appearing in the central martensite bands. The coalescence is mainly dominated by void sheet mechanism. The minimum thickness in this section is 0.62mm which corresponds to an average strain of 95.6%, which is slightly higher than the maximum strain level obtained from the ARAMIS measurements. Fig. 6 shows the SEM image taken in the center of the cut made perpendicular to the loading direction. It shall be realized that the long martensite bands are located out of plane in this image. Coalescence is occurring in the central region along the thickness. Most probably this coalescence is occurring among the voids in adjacent long central martensite bands. This coalescence will initiate a meso-crack in the central thickness which is perpendicular to the loading direction. Hardly any damage was observed in the cut near the edge of the specimen width. The thickness in the center (0.64mm) of the specimen is smaller than at the edge of the specimen (0.86mm).

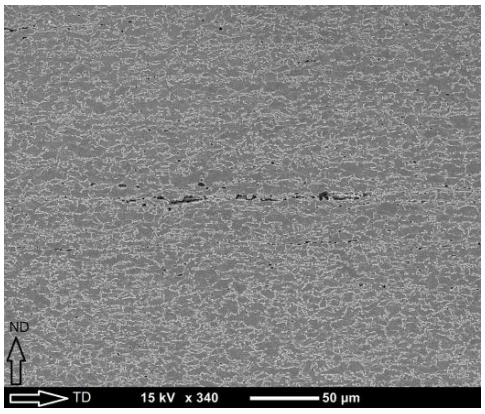

Fig. 6 *Sample cut ⊥ to the loading direction.*

3.2.2 Specimens Loaded in 90° to RD

Fig. 7 shows the SEM image in the central region along the thickness for the sample cut along the loading direction. Voids are well distributed in this section. Coalescence was not observed in this sample. Another sample was cut along the localized neck (Fig. 8). Voids are distributed uniformly along the neck throughout the thickness.

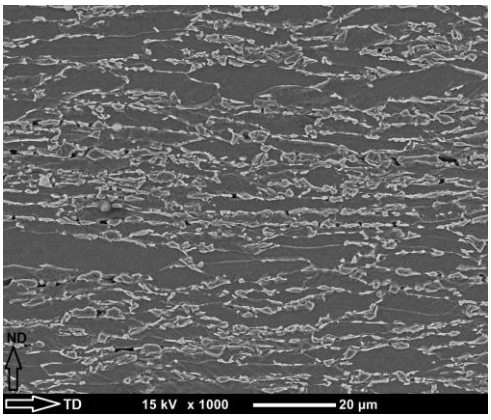

Fig. 7 *Sample cut ∥ to the loading direction.*

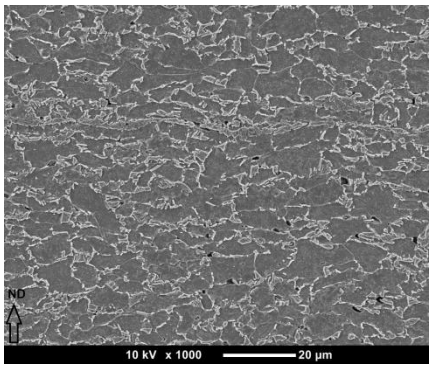

Fig. 8 *Sample cut along the localized neck.*

3.3 BROKEN SAMPLES

The specimens shown in Fig. 3 were used in this analysis. First the fracture surface was examined and then the specimens were cut along the loading direction, crossing the section with minimum thickness.

3.3.1 Specimen Loaded in 0° to RD

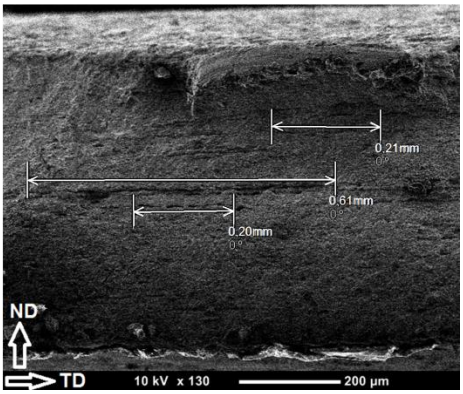

Fig. 9 *Fracture surface of specimen in Fig. 3(a).*

The fracture surface of the broken specimen shown in Fig. 3(a) was inspected with the SEM. The minimum thickness obtained in the fracture surface was 0.58mm and the thickness at the edge of the specimen was found to be 0.78mm. The large variation in the thickness is due to the fact that the fracture does not follow the localized bands. The minimum thickness of 0.58mm corresponds to an equivalent plastic strain of 108.9%. Fig. 9 shows the SEM image of the fracture surface which covers the complete thickness. Void coalescence can be observed in the central region of the image. This coalescence cannot be observed in the fracture regions towards the edges of the specimen. Apart from the small protruded region in the top and the long void coalescence in the central region, the rest of the fracture surface is dominated by shear failure. The SEM image of the section through the fracture surface is shown in Fig. 10. The void density in the long central martensite band and the void coalescence can be observed from this image as well.

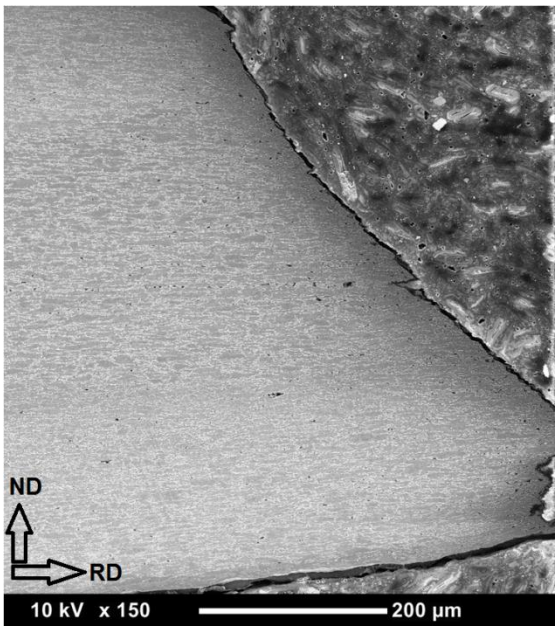

Fig. 10 *Section across fracture surface.*

3.3.2 Specimen Loaded in 90^o to RD

The fracture surface of the broken specimen shown in Fig. 3(b) was inspected with the SEM. A constant thickness is obtained along the fracture length (~0.45mm), which corresponds to an equivalent plastic strain of 159.7%. Fig. 11 shows the SEM image of the fracture surface which covers the complete thickness. Large voids can be observed throughout the fracture surface along the thickness. These large voids are slightly more concentrated towards the center. Void coalescence by void impingement is observed at various locations throughout the fracture surface. The section taken across the fracture surface showed well distributed voids throughout the thickness. A cup cone failure mode was observed. This specimen failed dominantly in a ductile mode.

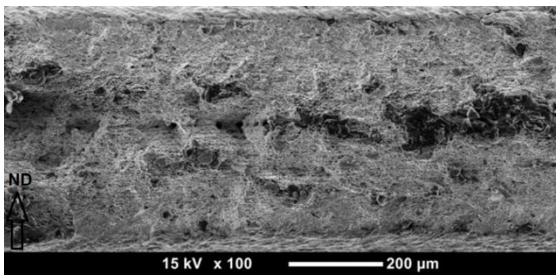

Fig. 11 *Fracture surface of specimen in Fig. 3(b).*

3.4 DISCUSSION

This DP600 material does have anisotropic martensite morphology in the form of continuity and size of martensite bands. Although this anisotropy does not have an influence in the initial and middle stages of tensile deformation. However it induces different deformation and damage characteristics in the later stages of deformation i.e. just before final failure.

In the specimens loaded in RD, the martensite bands are approximately of the same size as the localization length scale. Therefore upon localization, further deformation can occur only if the martensite bands will break. Since the triaxiality is higher in the center of the localized neck compared to the edges, therefore the probability of void initiation in the center of the localized band is higher. Fracture of these long martensite bands in the central region of the localized band creates a high gradient of stiffness from the center to the edges, where the long bands are still intact. The gradient in the stiffness gives rise to a gradient in the strain across the localized band and thus a large variation in thickness. The voids initiated in the long martensite bands are concentrated in the center of the thickness. This promotes coalescence of voids in neighboring bands by void sheet mechanism perpendicular to the loading direction. The coalescence only occurs in the central region of the localized band because at the edges there are not much voids to coalesce. After coalescence in the center of the thickness, the rest of the material fails in a brittle manner i.e. shear failure mode, perpendicular to the loading. The early void coalescence by void sheet mechanism reduces the formability of the material when loaded along the RD.

On the other hand, the material has shorter martensite bands in 90^o to RD. These bands do not have an influence till the very end of the deformation and therefore the voids are much more distributed throughout the localized neck and thickness. The voids get enough time to grow and coalesce by void impingement. Therefore the material fails in a ductile manner and has larger formability when loaded 90^o to RD.

4 MODELING OF MIAD

The Modified Lemaitre's (ML) anisotropic damage model, presented in [2], is a continuum damage model based on the hypothesis of strain equivalence [4]. This model accounts for LIAD only. Few damage models do define direction dependent damage parameters in their models but those parameters are based on the elastic/plastic anisotropy of the material [5] or by determining the crack density distribution [6]. In this work the ML anisotropic damage model was adapted to include MIAD in a phenomenological way. Eq. 1 presents the damage evolution law for the model.

$$\dot{\tilde{D}} = C \cdot \left(\frac{\tilde{\sigma}_{eq}^2 \cdot \tilde{R}_v}{2 \cdot E \cdot S_c} \right)^s \left| \bar{\bar{A}} : \dot{\bar{\varepsilon}}_p \right| \qquad (1)$$

Where $\vec{D}$ is a second order damage tensor, $\tilde{\sigma}_{eq}$ is the effective equivalent stress, $\tilde{R}_v$ is a triaxiality factor, E is the Young's modulus, S_c is a triaxiality dependent damage parameter, $\vec{\varepsilon}_p$ is the plastic strain tensor, s is a strain rate dependent damage parameter and $\vec{\vec{A}}$ is a fourth order MIAD tensor given as follows:

$$\vec{\vec{A}} = f\left(A_0, A_{45}, A_{90}\right) \tag{2}$$

A_0, A_{45} and A_{90} are three scalar parameters determined from tensile tests carried out in 0°, 45° and 90° directions.

$$A_{0,45,90} = \frac{D_l}{D_t} \tag{3}$$

Where D_l and D_t are damage components in the lateral and thickness direction. The MIAD tensor $\vec{\vec{A}}$ changes the ratio of the damage distribution in different directions but it does not change the overall damage depending upon the orientation of material with respect to loading. C is a scalar MIAD function, dependent upon loading angle with respect to RD. This function is incorporated to scale up or scale down the damage evolution rate depending upon the loading direction with respect to the material direction i.e. θ. The function C is selected as a quadratic function:

$$C(\theta) = A_1 \cdot \theta^2 + A_2 \cdot \theta + A_3 \tag{4}$$

Where A_1, A_2 and A_3 are fitting parameters.

4.1 MIAD PARAMETERS

There are six MIAD parameters which have to be determined i.e. A_0, A_{45} and A_{90} for the MIAD tensor $\vec{\vec{A}}$ and A_1, A_2 and A_3 for the scalar function C. The determination of MIAD parameters A_0, A_{45} and A_{90} require damage measurements in lateral and thickness direction in tensile tests loaded in 0°, 45° and 90° to RD. Direction dependent quantitative damage measurements are not performed in this study therefore the parameters A_0, A_{45} and A_{90} are taken equal to 1.

The parameters A_1, A_2 and A_3 have to be fitted to the tensile tests carried out in 0°, 45° and 90° to RD. The mean failure strain values (based on gauge length of 50mm) and the deviation around the mean for the tensile tests in the three directions are shown in Fig. 12. The highest deviation is found for the specimens loaded in 45° to the RD. This large deviation is understandable as the long martensite bands are inclined to the loading direction and the failure can be governed by either shear failure, or ductile failure or even a mixed failure mode. Due to the large variation in the results in the tensile tests loaded in 45° to RD, a linear function for C would suffice in this case i.e. $A_1 = 0$ (see Fig. 12). The remaining two parameters i.e. A_2 and A_3 were fitted to the mean post localized regime of the engineering stress strain curves, obtained from the tensile tests loaded in 0° and 90° to RD. The values were found to be $A_2 = -1.1$ and $A_3 = 1.2$.

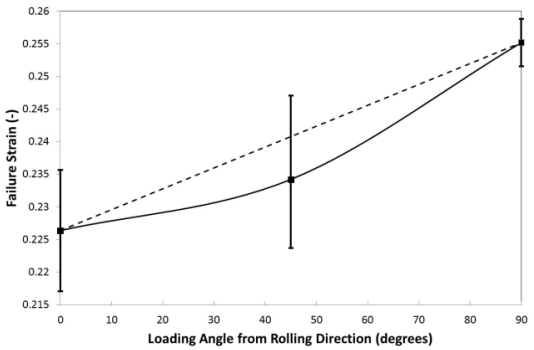

Fig. 12 *Mean failure strain as a function of θ.*

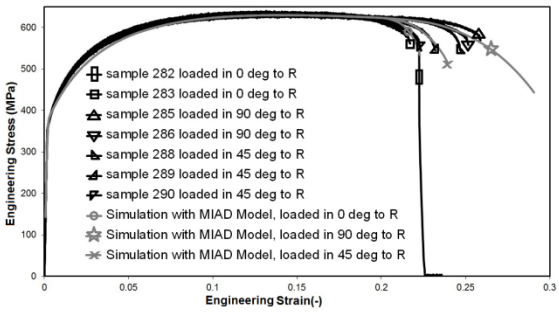

Fig. 13 *Experiments vs. simulations.*

4.2 RESULTS AND DISCUSSION

Fig. 13 shows the comparison of the engineering stress strain curves obtained from the simulation and experiments. It can be observed that the stress strain curves obtained from the simulations follow the post localization regime of the experimental curves for the three directions. Despite of the good comparison in the post localization curves, the stress and strain at which the simulation fails, is not in a good comparison with the experiments. The reason is that the model includes MIAD in the rate of damage growth (void growth) but the damage initiation threshold and the critical damage at which failure occurs is equal for all directions. Therefore in the simulation, loaded in the 90° to the RD, damage begins at the same strain level as in the other directions (i.e. 0.18) but the damage grows at a much slower rate. Since the critical damage value is also the same for all directions (i.e. 0.179), the simulation loaded in the 90° to the rolling direction fails at a much lower stress and higher strain. Including MIAD in damage initiation and critical damage value will complicate the mod-

el, as additional material parameters have to be incorporated in the model.
The deformation, damage and failure behavior observed in experiments are not observed in the simulations. Homogenized material properties are assumed throughout the thickness in this model which is in contradiction to the basis on which the failure mechanisms in Section 3.4 were explained. So, if the material failure mode is dominated by the non-uniform underlying microstructure then the MIAD model may not predict the failure mode correctly.

5 CONCLUSIONS AND DISCUSSION

It was shown that the phenomenon of MIAD exists in a pre-production DP600 steel grade. MIAD can be an important phenomenon in advanced high strength steels. Ignoring MIAD can produce misleading conclusions about the material characteristics which will consequently end in faulty manufacturing process designs and product designs. On the other hand, considering MIAD, in these materials, can be an advantage in the sense that material orientation can be utilized for efficient manufacturing process designs. Table 1 shows the extent up to which MIAD can influence the deformation, damage and failure behavior of the material. A MIAD model was developed to account for the differences in damage growth within the framework of continuum damage mechanics. The model was capable to predict the post localization engineering stress strain behavior of the material. This is a first step towards incorporation of MIAD in continuum damage models. Further developments are required in the modeling of MIAD phenomenon. Translation of the influence of second phase anisotropy (martensite morphology) to continuum damage via the MIAD parameters will be one of the most important future research areas in MIAD modeling. Complete details of the metallographic study of MIAD, the MIAD model and parameter identification can be found in [7].
It is worth to mention here that the phenomenon of MIAD is not only dependent upon the martensite morphology but also upon the loading conditions and the strain rate. As an example, no MIAD was observed in the cross die drawing tests in [2], because the damage and deformation develops from the outer surface of the sheet and not from the mid where the long martensite bands were present. The martensite morphology, which is very important in a tensile loading, may not be important under bending. It was also observed that increasing the strain rate may have an influence on how damage develops and failure propagates [7].
Manufacturing of DP steels of thickness 1mm or higher with a uniformly distributed martensite is not a trivial task. Even if it is trivial, producing such kind of steel on commercial basis would not be feasible. The best option currently available is to study the influence of this inhomogeneity and use it to our best. This research is an initial effort in determining the phenomenon of MIAD and its influence on material characterization.

Table 1: *Summary of experimental findings.*

Loading	**0^o to RD**	**90^o to RD**
Martensite band length in mid plane thickness	~1mm	~200µm
Engineering ϵ_f	~23%	~26%
Max. True ϵ_f	~108%	~160%
Void Distribution	Concentrated in center	Uniform
Coalescence Mechanism	Void sheet	Void impingement
Thickness along fracture	0.78~0.58mm	~0.45mm
Dominant failure mode	Shear failure	Ductile failure

6 ACKNOWLEDGEMENT

This research was carried out under the project number M61.1.08308 in the framework of the Research Program of the Materials innovation institute (M2i) (www.M2i.nl).

REFERENCES

[1] Krajcinovic D.: *Damage mechanics*. North-Holland, Amsterdam, 1996.
[2] Niazi M.S., Wisselink H.H., Meinders T., Huétink J.: *Failure predictions for dp steel cross-die test using anisotropic damage*. International Journal of Damage Mechanics, DOI: 10.1177/1056789511407646, 2011.
[3] Avramovic-Cingara G., Ososkova Y., Jain M.K., Wilkinson D.S.: *Effect of marten-site distribution on damage behavior in DP600 dual phase steels*. Materials Science and Engineering A, 516:7–16, 2009.
[4] Lemaitre J., Desmorat R.: Engineering Damage Mechanics. Springer, 2005.
[5] Shen W., Peng L.H., Tang C.Y.: *An anisotropic damage-based plastic yield criterion and its application to analysis of metal forming process*. International Journal of Mechanical Sciences, 47:1897–1922, 2005.
[6] Hammi Y., Horstemeyer M.F.: *A physically motivated anisotropic tensorial representation of damage with separate functions for void nucleation, growth and coalescence*. International Journal of Plasticity, 23:1641–1678, 2007.
[7] Niazi M.S., Wisselink H.H., Meinders T., van den Boogaard A.H.: *Material Induced Anisotropic Damage*. In preparation.